Highly Polarized Photoluminescence and Photodetection from Single Indium Phosphide Nanowires

Jianfang Wang,[1]* Mark S. Gudiksen,[1]* Xiangfeng Duan,[1] Yi Cui,[1] Charles M. Lieber[1,2]†

We have characterized the fundamental photoluminescence (PL) properties of individual, isolated indium phosphide (InP) nanowires to define their potential for optoelectronics. Polarization-sensitive measurements reveal a striking anisotropy in the PL intensity recorded parallel and perpendicular to the long axis of a nanowire. The order-of-magnitude polarization anisotropy was quantitatively explained in terms of the large dielectric contrast between these free-standing nanowires and surrounding environment, as opposed to quantum confinement effects. This intrinsic anisotropy was used to create polarization-sensitive nanoscale photodetectors that may prove useful in integrated photonic circuits, optical switches and interconnects, near-field imaging, and high-resolution detectors.

Optical studies of one-dimensional (1D) nanostructures have focused primarily on lithographically and epitaxially defined quantum wires (*1*–*5*) embedded in a semiconductor medium. Free-standing nanowires have several attractive differences from these systems, including a large variation in the dielectric constant of the surrounding media and a cylindrical, strongly confining potential for both electrons and holes. Here we report optical studies of individual free-standing InP nanowires that demonstrate giant polarization anisotropy in PL measurements and the use of these InP nanowires as photoconductivity (PC)-based photodetectors. We synthesized single-crystal InP nanowires via a laser-assisted catalytic growth (LCG) method described previously (*6*–*8*). Monodisperse nanowire samples with diameters of 10, 15, 20, 30, and 50 nm were suspended in ethanol solution and later were dispersed onto quartz substrates for PL measurements. Atomic force microscopy images show that individual and well-isolated nanowires are readily produced by this method (Fig. 1A). To probe the PL and PC properties of a single InP nanowire, we used a home-built, far-field epifluorescence microscope equipped with a charge-coupled device (CCD) and spectrometer to image and obtain luminescence spectra (*9*). In this way, we avoid the averaging inherent in ensemble experiments (*5*, *10*).

PL images of single InP nanowires recorded at room temperature with the polarization of the exciting laser parallel (Fig. 1B) and perpendicular (Fig. 1C) to the nanowire show a giant polarization anisotropy. Essentially, the observed PL turns from "on" to "off" as the excitation polarization is rotated from parallel to perpendicular. Integration of the emission as a function of excitation angle shows that the intensity exhibits a periodic ($\cos^2\theta$) dependence on angle (Fig. 1, inset). From the nanowire PL image (Fig. 1B), it is also evident that the emission intensity is relatively uniform along the wire axis.

We recorded PL spectra (*11*, *12*) from a number of individual wires as a function of excitation (Fig. 2A) or emission (Fig. 2B) polarization. In both cases, the ratio of parallel to perpendicular emission is greater than an order of magnitude. The order-of-magnitude polarization anisotropy is exhibited over most of the energy range of the PL peak (insets of Fig. 2, A and B) and for excitation with both 488- and 514-nm laser wavelengths. On average, the measured excitation and emission polarization ratios, $\rho = (I_{//} - I_{\perp})/(I_{//} + I_{\perp})$, of the intensities parallel ($I_{//}$) and perpendicular ($I_{\perp}$) to the wire axis are 0.91 ± 0.07. Many nanowires exhibited a polarization ratio of 0.96. The polarization ratio was independent of nanowire diameter between 10 and 50 nm, but radial quantum confinement effects were observed for diameters ≤20 nm.

The ratio of PL intensities ($I_{//}/I_{\perp}$) is at least 10 times greater than the ratio for previously reported quantum wire samples (*2*–*4*). Polarization anisotropy in quantum wires has been attributed to the mixing of valence bands due to quantum confinement. This quantum mechanical effect yields substantially smaller polarization ratios ($\rho < 0.60$) than we observed. In our case, the large polarization response can be accounted for in terms of the large dielectric contrast between the nanowire and its air or vacuum surroundings. We have modeled this effect quantitatively by treating the nanowire as an infinite dielectric cylinder in a vacuum, because the wavelength of the exciting light is much greater than the wire diameter (Fig. 2C). When the incident field is polarized parallel to the cylinder, the electric field inside the cylinder is not reduced. But when polarized perpendicular to the cylinder, the electric field amplitude is attenuated according to

$$E_i = \frac{2\varepsilon_0}{\varepsilon + \varepsilon_0} E_e \qquad (1)$$

where E_i is the electric field inside the cylinder, E_e the excitation field, and ε (ε_0) is the dielectric constant of the cylinder (vacuum) (*13*). Using the dielectric constant for bulk InP of 12.4, we calculate a theoretical polarization ratio, $\rho = 0.96$, which is in excellent agreement with the maximum values determined in our experiments.

These calculations show that classical electromagnetic theory accounts well for the observed polarization anisotropy and suggest that quantum effects do not contribute substantially. Moreover, these results suggest that by tailoring the environment around a nanowire, for example, by adsorption of molecules or growth of inorganic layers with varying dielectric properties, it will be possible to modify systematically the polarization response in a way not possible for surface-grown quantum wires.

The extreme PL polarization anisotropy of these InP nanowires suggests that they could serve as photodetectors, optically gated switches, and light sources, and we have fabricated polarization-sensitive photodetectors in which an individual nanowire serves as the device element (Fig. 3A). Nanowires were dispersed onto silicon substrates, and electrical contacts were defined at the nanowire ends with the use of electron beam lithography and followed by thermal evaporation of the metal electrodes. The nanowire devices were then placed in the epifluorescence microscope used for PL imaging, and the change in conductance (G) of the nanowires was measured via lock-in technique as a function of the laser intensity and polarization.

In general, the conductance of individual nanowires increased by two to three orders of magnitude (Fig. 3B) with increasing excitation power density. The PC is reproducible and reversible with respect to changes in the excitation power. This response suggests that the increases are due to direct carrier collection at the nanowire–metal contact interface versus population of surface traps, which would effectively gate the nanowire. The

[1]Department of Chemistry and Chemical Biology, [2]Division of Engineering and Applied Sciences, Harvard University, Cambridge, MA 02138, USA.

*These authors contributed equally to this work.
†To whom correspondence should be addressed. E-mail: cml@cmliris.harvard.edu

PC also shows a striking polarization anisotropy with parallel excitation producing G that is over an order of magnitude larger than perpendicular excitation (Fig. 3B). The photoconductivity anisotropy ratio, $\sigma = (G_{//} - G_{\perp})/(G_{//} + G_{\perp})$, where $G_{//}$ ($G_{\perp}$) is the conductance with parallel (perpendicular) excitation, is 0.96 for the shown device (Fig. 3B, inset), in excellent agreement with the polarization ratio measured from PL. The reproducibility of the PC polarization response is explicitly seen in plots of conductance recorded as the excitation polarization vector is continuously rotated (Fig. 3C). We also note that the PC polarization anisotropy is expected to be nearly wavelength-independent for energies larger than the nanowire band gap. By making a cross of two nanowires (*14*–*16*) and independently measuring their PCs, one could make a device to simultaneously measure intensity and polarization.

Moreover, the active device element in our nano-photodetector is substantially smaller than other polarization-sensitive quantum well-based detectors (*17*, *18*), which are not smaller than 50 μm by 50 μm and are often sensitive to only one wavelength of light.

To gauge the sensitivity of these photodetectors, we determined that the responsivities are as high as 3000 amperes/watt (A/W) as a figure of merit. This represents a high value for our unoptimized device (*19*), and we believe that investigations of nanowire composition and contacts should lead to further improvements. For example, InP nanowire detectors incorporating Ge traps exhibit responsivities up to 10,000 A/W, although this comes at a cost of reduced detector speed. In addition, these extremely small devices open the possibility of creating high-speed detectors (*20*, *21*).

Nanowire photodetectors could be exploited as optically gated switches, used to create very high-density optical interconnects, and incorporated into photonic-based circuits, where polarization detection could vastly increase the information bandwidth. Combined with the ability to synthesize nanowires out of virtually any group IV, III-V, or II-VI semiconductor material (*6*), we believe that this work opens up exciting opportunities for the creation of a wide range of detectors and high-resolution detector arrays for different spectral regimes, including the 1.5-μm regime important in current optical communications.

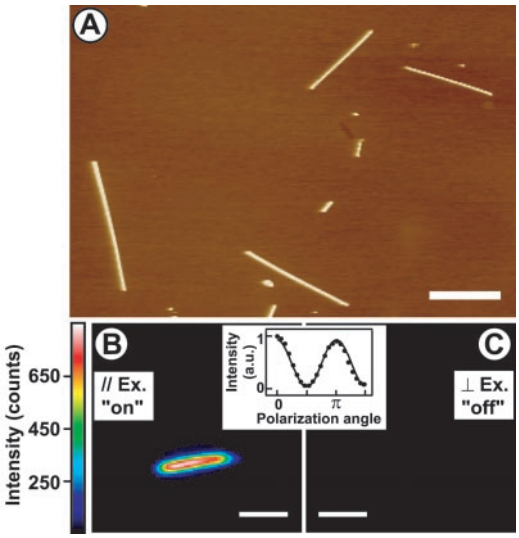

Fig. 1. PL characterization of InP nanowires. (**A**) Atomic force microscopy image of nanowires dispersed on a substrate for PL measurements, showing that the individual nanowires are monodisperse and well separated from one another on the surface. Scale bar, 5 μm. (**B**) PL image of a single 20-nm InP nanowire with the exciting laser polarized along the wire axis. Scale bar, 3 μm. (**C**) PL image of the same nanowire as in (B) under perpendicular excitation. Intensity scale is identical to (B). Inset, variation of overall photoluminescence intensity as a function of excitation polarization angle with respect to the nanowire axis. The PL images were recorded at room temperature with integration times of 2 s.

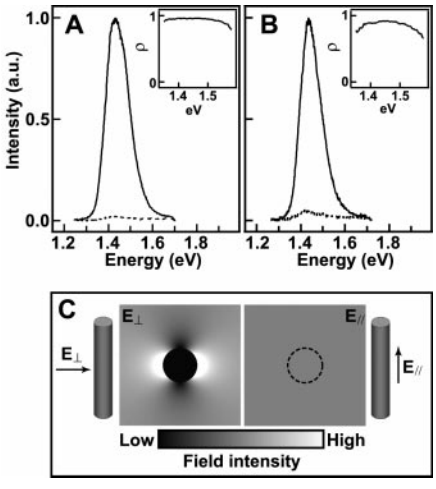

Fig. 2. Polarized excitation and emission spectra of nanowires. (**A**) Excitation spectra of a 15-nm-diameter InP nanowire. These spectra were recorded with the polarization of the exciting laser aligned parallel (solid line) and perpendicular (dashed line) to the wire axis. The polarization ratio, ρ, is 0.96. Inset, plot of the polarization ratio as a function of energy. (**B**) Emission spectra of the same wire as in (A). These spectra were taken with the excitation parallel to the wire, while a polarizer was placed in the detection optics. The polarization ratio of the parallel (solid line) to perpendicular (dashed line) emission is 0.92. The spectra were taken with integration times of 10 s. Inset, plot of the polarization ratio as a function of energy. (**C**) Dielectric contrast model of polarization anisotropy. The nanowire is treated as an infinite dielectric cylinder in a vacuum while the laser polarizations are considered as electrostatic fields oriented as depicted. Field intensities ($|\boldsymbol{E}|^2$) calculated from Maxwell's equations clearly show that the field is strongly attenuated inside the nanowire for the perpendicular polarization, $\boldsymbol{E}_{\perp}$, whereas the field inside the nanowire is unaffected for the parallel polarization, $\boldsymbol{E}_{//}$.

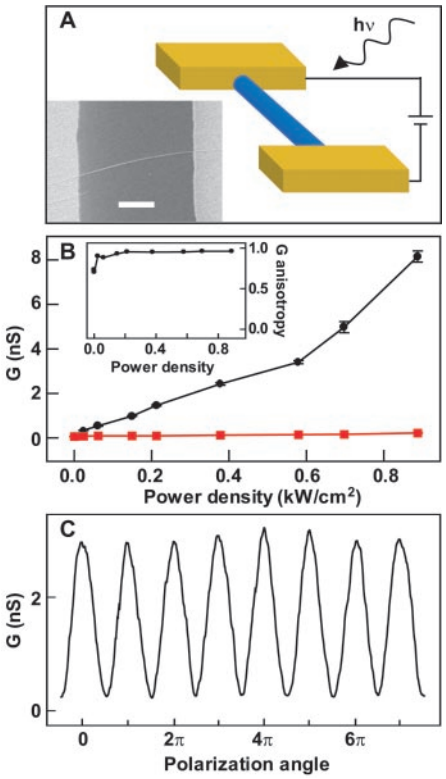

Fig. 3. Polarized photodetection using individual InP nanowires. (**A**) Schematic depicting the use of a nanowire as a photodetector by measuring the change in PC as a function of incident light intensity and polarization. Inset, field-emission scanning electron microscopy image of a 20-nm-diameter nanowire and contact electrodes for PC measurements. Scale bar, 2 μm. Nanowires were first dispersed in ethanol and then deposited onto silicon substrates (600-nm oxide, 1 to 10 ohm-cm resistivity). Electrical contacts to the wires were defined using electron beam lithography, and Ni/In/Au contact electrodes were thermally evaporated. (**B**) Conductance, G, versus excitation power density. Shown is the PC response when the illumination is polarized parallel (black) and perpendicular (red) to the wire. Inset, PC anisotropy, σ, versus excitation power calculated from (B). The measured anisotropy for the shown device is 0.96. (**C**) Conductance versus polarization angle as the polarization was manually rotated while measuring the PC. All PC measurements were done at room temperature. Current collected at drain electrode was measured using standard lock-in techniques, with an excitation voltage of 50 mV at 31 Hz. No gate voltage was applied. An excitation wavelength of 514.5 nm was used for these measurements.

References and Notes

1. T. Someya, H. Akiyama, H. Sakaki, *Phys. Rev. Lett.* **74**, 3664 (1995).
2. F. Vouilloz *et al.*, *Phys. Rev. B* **57**, 12378 (1998).
3. H. Akiyama, T. Someya, H. Sakaki, *Phys. Rev. B* **53**, R4229 (1996).
4. P. Ills *et al.*, *Phys. Rev. B* **51**, 4272 (1995).
5. J. Hasen *et al.*, *Nature* **390**, 54 (1997).
6. X. Duan, C. M. Lieber, *Adv. Mater.* **12**, 298 (2000).
7. M. S. Gudiksen, C. M. Lieber, *J. Am. Chem. Soc.* **122**, 8801 (2000).
8. M. S. Gudiksen, J. Wang, C. M. Lieber, *J. Phys. Chem. B* **105**, 4062 (2001).
9. Excitation light (488 or 514 nm) was focused by an objective (NA = 0.7) to a ~30-μm diameter spot at ~1.0 kW/cm^2 on the quartz substrate with nanowires dispersed on it. A λ/2 wave plate was used to change the polarization of excitation light. The resulting PL was collected by the same objective, filtered to remove excitation light, focused, and either imaged or spectrally dispersed onto a liquid nitrogen–cooled CCD. To determine the emission polarization, a Glan-Thompson polarizer was placed in front of the spectrometer to detect emission intensities.
10. S. A. Empedocles, D. J. Norris, M. G. Bawendi, *Phys. Rev. Lett.* **77**, 3873 (1996).
11. PL spectra exhibit a diameter-dependent shift in the PL emission energy from the bulk band gap of InP (1.35 eV) for diameters ≤20 nm. Detailed studies show that diameter-dependent spectra collected from nanowires at room temperature and ~7 K can be explained in terms of radial quantum confinement. Giant polarization anisotropy is observed in nanowires with diameters from 10 to 50 nm at room temperature and 7 K.
12. M. S. Gudiksen, J. Wang, C. M. Lieber, in preparation.
13. L. D. Landau, E. M. Lifshitz, L. P. Pitaevskii, *Electrodynamics of Continuous Media* (Pergamon, Oxford, 1984), pp. 34–42.
14. X. Duan, Y. Huang, Y. Cui, J. Wang, C. M. Lieber, *Nature* **409**, 66 (2001).
15. Y. Huang, X. Duan, Q. Wei, C. M. Lieber, *Science* **291**, 630 (2001).
16. Y. Cui, C. M. Lieber, *Science* **291**, 851 (2001).
17. S. Ura, H. Sunagawa, T. Suhara, H. Nishihara, *J. Lightwave Tech.* **6**, 1028 (1988).
18. C. J. Chen, K. K. Choi, L. Rokhinson, W. H. Chang, D. C. Tsui, *Appl. Phys. Lett.* **74**, 862 (1999).
19. M. Bass *et al.*, *Handbook of Optics* (McGraw Hill, New York, 1995), pp. 17.1–17.29.
20. These very small devices could prove useful for high-speed detection because the response times of semiconductor photodetectors can be limited by their resistance-capacitance (RC) time constants (*19*). On the basis of improved nanowire–metal contacts (10 kilohm) and intrinsically small capacitances (~10^{-17} F) (*21*), RC time constants on the order of 100 fs can be realized. By decreasing the electrode separation to ensure direct collection of photogenerated carriers, detection speeds on the order of 100 fs or less may be realized with these nanoscale detectors.
21. Y. Cui, X. Duan, J. Hu, C. M. Lieber, *J. Phys. Chem. B* **104**, 5213 (2000).

22. We thank L. Lauhon and H. Park for helpful discussions. M.S.G. thanks the NSF for predoctoral fellowship support. C.M.L. acknowledges support of this work by the Office of Naval Research and Defense Advanced Projects Research Agency.

8 May 2001; accepted 24 August 2001

Time-Resolved Measurement of Dissipation-Induced Decoherence in a Josephson Junction

Siyuan Han,[1]* Yang Yu,[1] Xi Chu,[2] Shih-I Chu,[2] Zhen Wang[3]

We determined the dissipation-induced decoherence time (DIDT) of a superconducting Josephson tunnel junction by time-resolved measurements of its escape dynamics. Double-exponential behavior of the time-dependent escape probability was observed, suggesting the occurrence of a two-level decay-tunneling process in which energy relaxation from the excited to the ground level significantly affects the escape dynamics of the system. The observation of temporal double-exponential dependence enables direct measurements of the DIDT, a property critical to the study of quantum dynamics and the realization of macroscopic quantum coherence and quantum computing. We found that the DIDT was $\tau_d > 11$ μs at $T = 0.55$ K, demonstrating good prospects for implementing quantum computing with Josephson devices.

Use of solid-state devices (SSD) is regarded as one of the most promising approaches for the development of quantum computers (QC), due to the relative ease of circuit design, fabrication, and scaling up (*1–10*). However, coupling between SSD and the environment results in dissipation, and hence decoherence. Here, decoherence refers to processes that lead to exponential decay of superposition states into incoherent mixtures. The severity of decoherence is characterized by the decoherence time—the time constant τ of the exponential decay. Both dissipation (with decoherence time τ_d) and phase relaxation (with τ_φ) lead to decoherence (*11–15*). Realization of QC will depend critically on our ability to create and preserve coherent superposition states so that decoherence presents the most fundamental obstacle (*11–16*). One way to increase the decoherence time in SSD is to use superconducting qubits (SQ) based on superconducting quantum interference devices (SQUIDs) (flux qubits) or single-pair tunneling devices (charge qubits) (*3–10*). For both types of SQ, the Josephson junction is the key element and it is the dissipation of the junctions that will set the limit on decoherence time. Furthermore, for SQUID qubits τ_d^{-1} and τ_φ^{-1} are predicted to be proportional to the level of dissipation (*17, 18*). Therefore, the feasibility of implementing QC with SQ depends on whether dissipation in Josephson junctions can be made sufficiently low to keep the error rate to a tolerable level. However, experimental determination of either τ_d or τ_φ is extremely difficult for superconducting devices because in each measurement only a single device, rather than an ensemble of identical devices, is available for signal detection. Furthermore, prior to this work no time-domain measurement with resolution comparable to the decoherence time scale of SQ has been demonstrated. For these reasons, no time-resolved measurement of τ_d (or τ_φ) has been reported yet. Recent attempts to determine the effective damping resistance of a Josephson junction in a SQUID were inconclusive due to the questionable method of data analysis used and the indirect nature of the measurement technique (*19, 20*). We present time-resolved measurements of τ_d in a NbN/AlN/NbN Josephson junction. The measured decoherence time, $\tau_d > 10$ μs at $T = 0.55$ K, corresponds to a qubit quality factor $\tau_d/\tau_{op} \sim 10^4$ (where $\tau_{op} \sim 1$ ns is the typical gate time of SQUID qubits), demonstrating strong potential for QC employing NbN SQUID qubits (*12*).

The equation of motion for a current biased Josephson junction, $Cd^2\Phi/dt^2 + R^{-1}d\Phi/dt = -\partial U/\partial\Phi$, is homologous to that of a particle of mass C moving in a washboard potential $U(\Phi) = -I_b\Phi - E_J\cos(2\pi\Phi/\Phi_0)$ with damping constant R^{-1}, where C is the junction capacitance, R is the shunt resistance, $\Phi_0 \equiv h/2e$ is the flux quantum, $E_J \equiv I_c\Phi_0/2\pi$ is the magnitude of maximum Josephson coupling energy, I_c is the critical current of the junction, I_b is the bias current, and $\Phi \equiv (\varphi/2\pi)\Phi_0$, where φ is the phase difference across the junction. For $i_b \equiv I_b/I_c < 1$, the potential has a series of metastable wells. The dc voltage across the junction is zero when the particle is trapped in a potential well. The depth of the potential well decreases as i_b is increased and becomes zero for $i_b \geq 1$. In the presence of thermal/quantum fluctuations, a junction initially trapped in the zero-voltage state can escape from the potential well to enter the finite-voltage state.

Previous experiments have demonstrated

[1]Department of Physics and Astronomy, University of Kansas, Lawrence, KS 66045, USA. [2]Department of Chemistry, University of Kansas, Lawrence, KS 66045, USA. [3]Kansai Advanced Research Center, Communication Research Laboratory, Ministry of Posts and Telecommunications, 588-2 Iwaoka, Iwaoka-cho, Nishi-ku, Kobe, 651-24 Japan.

*To whom correspondence should be addressed. E-mail: han@ku.edu